International Conference on Applied Energy 2019
Aug 12-15, 2019, Västerås, Sweden
Paper ID:

A NOISE COMPENSATED METHOD FOR MODEL PARAMETERIZATION OF LITHIUM-ION BATTERY

Zhongbao Wei[1], Hongwen He [1*]

1 National Engineering Laboratory for Electric Vehicles, School of Mechanical Engineering, Beijing Institute of Technology, China

ABSTRACT

A well-parameterized battery model is prerequisite of the model-based estimation and control methods. This paper focuses on the unbiased model parameter identification when noises corrupt the measurements. The parameter identification problem within the noise corruption scenario is reformulated as a nonlinear least squares (NLS) problem. A novel offline two-step method combining least squares (LS) regression and variable projection algorithm (VPA) is then proposed to co-estimate the noise variances and unbiased model parameters. The proposed LSVPA is further extended to the online recursive version by using the Gauss-Newton (GN) method. Simulation and experimental results show that the proposed method can well compensate for the noise effect and improve the accuracy of model parameterization.

Keywords: lithium-ion battery, model parameter identification, noise compensation, variable projection

1. INTRODUCTION

Lithium-ion batteries (LIBs) have been widely used for electric vehicles (EVs), while a reliable battery management system (BMS) is indispensable to improve the safety and life expectancy of LIB systems.

The model-based management has been widely studied over years due to the merit of high accuracy and robustness. Some typical applications include the model-based state estimation [1], fault diagnostic [2], and charge control [3]. Models for LIB can be broadly categorized into physics-based model [4], artificial intelligence model [5], and equivalent circuit model (ECM) [1]. Amongst others, the ECM has seen most applications for the structural simplicity and reasonable accuracy. However, the parameters of ECM are affected by many factors, which cause the ECM difficult to be parameterized, while an ill-parameterized model largely declines the model-based estimators or controllers.

The model parameter identification has been widely studied in the literature. The least squares (LS) and population-based optimization [6] are typically used for offline identification. In contrast, online identification can be achieved by methods like recursive least squares (RLS) [7] and extended Kalman filter (EKF) [8]. Such methods have been validated under laboratory condition. However, the acquired data in BMS contains unexpected noises which adversely affect the model identification. Noise-induced identification biases can be theoretically eliminated using bias compensating methods [9], but the knowledge of noise statistics is hardly known in practice. The total least squares (TLS)-based methods [10, 11] were proposed to attenuate the noise-induced parameterization biases. However, an approximate guess of the input and output noise level is required to give an accurate solution.

This paper focuses on the noise-immune model identification for LIB. The LS-based method is shown to be asymptotically biased if noises corrupt both system input and output. To address this problem, a novel method combining least squares (LS) regression and variable projection algorithm (VPA) is proposed to co-estimate the noise variances and unbiased model parameters. The recursive version of proposed LSVPA is also put forward for potential online utilization.

The rest of paper is organized as follows. Battery modeling and fundamental for parameter identification are presented in Section 2. The proposed noise-immune identification method is detailed in Section 3. Results are presented in Section 4, while conclusions are drawn in Section 5.

Selection and peer-review under responsibility of the scientific committee of the 11th Int. Conf. on Applied Energy (ICAE2019).

2. MODELING AND IDENTIFICATION

2.1 Battery Modeling

A general *n*-th order RC model as shown in Fig 1 is widely used for the BMS design. The voltage source describes the SOC-dependent OCV, while R_s is the ohmic resistance. The RC parallel branches aim to simulate polarization effects including charge transfer, diffusion, and passivation layer effect on electrodes. Governing equations of the *n*-th order RC model are given by:

$$C_{pi}\, dV_{pi}(t)/dt + V_{pi}(t)/R_{pi} = I_0(t) \tag{1a}$$

$$V_{t0}(t) = V_{oc}(t) - \sum_{i=1}^{n} V_{pi}(t) - I_0(t)R_s \tag{1b}$$

$$\dot{z}(t) = -\eta I_0(t)/Q \tag{1c}$$

where I_0 denotes the load current, V_{pi} the voltage across the *i*-th RC branch, V_{t0} the terminal voltage, z the SOC, η the coulomb efficiency, Q the maximum capacity. The OCV as a function of SOC are calibrated as:

$$V_{oc} = f(z) = \sum_{i=0}^{n_p} c_i z^i \tag{1d}$$

where c_i (i = 0, 1, 2, …, n_p) are the polynomial coefficients.

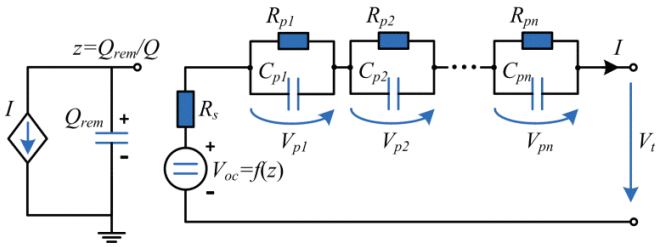

Fig 1 *n*-th order RC model for LIBs

2.2 Parameter Identification

The model parameters associated with Eqs. (1a)-(1c) should be identified accurately. Applying Laplace transform to Eqs. (1a)-(1b) gives:

$$\frac{y_0(s)}{I_0(s)} = -R_s - \sum_{i=1}^{n} \frac{R_{pi}}{1 + R_{pi}C_{pi}s} \tag{2}$$

where $y_0 = V_{t0} - V_{oc}$. Applying bilinear transform $s = 2(q-1)/t_s/(q+1)$ to (2) gives:

$$y_0(q^{-1})/I_0(q^{-1}) = -\sum_{i=0}^{n} b_i q^{-i} \Big/ (1 + \sum_{i=1}^{n} a_1 q^{-i}) \tag{3}$$

where q^{-1} is the backward shift operator. Rewriting Eq. (3) in the discrete-time domain gives:

$$y_{0,k} = \boldsymbol{\theta}_k^{\boldsymbol{T}} \boldsymbol{\varphi}_{0,k} \tag{4}$$

where $\boldsymbol{\vartheta} = [\boldsymbol{a}_k\ \boldsymbol{b}_k^{\boldsymbol{T}}]^{\boldsymbol{T}}$ with $\boldsymbol{a} = [a_1, a_2, \ldots, a_n]$ and $\boldsymbol{b} = [b_0, b_1 \ldots, b_n]^{\mathsf{T}}$, $\boldsymbol{\varphi}_{0,k} = [-y_{0,k-1}, \ldots, -y_{0,k-n}, I_{0,k}, I_{0,k-1}, \ldots, I_{0,k-n}]^{\mathsf{T}}$.

It is explicit that increasing the model order elevates the computing cost due to the cubic complexity of commonly used identification methods. In this paper, model order is determined as 1 considering the extra computing burden brought by the need of both online parameterization and state observation.

3. NOISE-IMMUNE PARAMETERIZATION

3.1 Error-in-Variables Analysis

The observations under noise corruption are:

$$I_k = I_{0,k} + \Delta I_k,\quad V_{t,k} = V_{t0,k} + \Delta V_{t,k} \tag{5}$$

where ΔI and ΔV_t are noises on I_0 and V_{t0}. The noises are assumed to be zero-mean, ergodic, and random with variances of σ_i and σ_v. The noises are also assumed to be mutually uncorrelated and independent from true values. Then the input and output of Eq. (4) become:

$$\boldsymbol{\varphi}_k = \boldsymbol{\varphi}_{0,k} + \Delta\boldsymbol{\varphi}_k \tag{6a}$$

$$y_k = V_{t0,k} + \Delta V_{t,k} - V_{oc,k} = y_{0,k} + \Delta V_{t,k} \tag{6b}$$

The noise corruption recast the solution of (4) a typical error-in-variable (EIV) problem.

Definition: The auto- and cross-covariance matrices of two vectors ($\boldsymbol{p}_k$ and $\boldsymbol{q}_k$) are defined by (7a). The cross-covariance vector between an vector ($\boldsymbol{p}_k$) and a scalar stochastic process (r_k) is defined by (7b), whilst the auto- and cross-covariance functions of two scalar stochastic processes (r_k and d_k) are defined by (7c).

$$\boldsymbol{R}_p = E\left[\boldsymbol{p}_k \boldsymbol{p}_k^T\right], \boldsymbol{R}_{pq} = E\left[\boldsymbol{p}_k \boldsymbol{q}_k^T\right] \tag{7a}$$

$$\boldsymbol{\xi}_{pr} = E\left[\boldsymbol{p}_k r_k\right], \boldsymbol{\xi}_{rp} = E\left[r_k \boldsymbol{p}_k^T\right] \tag{7b}$$

$$\boldsymbol{R}_r = E\left[r_k r_k\right], \boldsymbol{R}_{rd} = E\left[r_k d_k\right] \tag{7c}$$

where $E[\bullet]$ is the expected value operator.

With the corruption of noises, the compensated unbiased solution of Eq. (4) is given by [12]:

$$\boldsymbol{\theta}^* = \boldsymbol{R}_{\varphi_0}^{-1} \boldsymbol{\xi}_{\varphi_0 y_0} = (\boldsymbol{R}_{\varphi} - \boldsymbol{R}_{\Delta\varphi})^{-1} (\boldsymbol{\xi}_{\varphi y} - \boldsymbol{\xi}_{\Delta\varphi\Delta y}) \tag{8}$$

while the LS ignores the effect of noises and gives:

$$\boldsymbol{\theta}_{LS} = \boldsymbol{R}_{\varphi}^{-1} \boldsymbol{\xi}_{\varphi y} = \left(\boldsymbol{R}_{\varphi_0} + \boldsymbol{R}_{\Delta\varphi}\right)^{-1} \left(\boldsymbol{\xi}_{\varphi_0 y_0} + \boldsymbol{\xi}_{\Delta\varphi\Delta y}\right) \tag{9}$$

It is hence validated that the LS is asymptotically biased if the system input is disturbed with noises, due to the violation of underlying assumptions of LS.

3.2 Co-estimation of Parameters and Noise Variances

To eliminate the asymptotic bias of identification, the noise-induced covariance on system output and regressor has to be compensated. From this view, the parameterization problem can be reformulated as:

$$\boldsymbol{\xi}_{y\varphi}\boldsymbol{\theta} = \boldsymbol{R}_y - \sigma_v \tag{10a}$$

$$\left[\boldsymbol{R}_{\varphi} - \boldsymbol{R}_{\Delta\varphi}(\boldsymbol{\sigma})\right]\boldsymbol{\theta} = \boldsymbol{\xi}_{\varphi y} \tag{10b}$$

where it is clear that n_{θ}+1 equations are established and one degree of freedom (DOF) remains. Hence, a unique solution can be arrived provided additional constraints are introduced. The IV estimation is applied in this paper with following time shifted inputs as instruments:

$$\varsigma_k = \begin{bmatrix} I_{k-n_b} & I_{k-n_b-1} & \dots & I_{k-n_b-n_\varsigma+1} \end{bmatrix}^T \tag{11}$$

where n_{ς} is the number of additional inputs. Then the following constraint holds:

$$\boldsymbol{R}_{\varsigma\varphi}\boldsymbol{\theta} = \boldsymbol{\xi}_{\varsigma y} \tag{12}$$

Now we reformulate a new set of normal equations which is overdetermined. Define $\boldsymbol{w}_k = [y_k \quad \boldsymbol{\varphi}_k^T \quad \varsigma_k^T]^T$, combining Eqs. (10a), (10b) and (12) gives:

$$\left[\boldsymbol{R}_{w\varphi} - \boldsymbol{R}_{\Delta w\Delta\varphi}(\boldsymbol{\sigma})\right]\boldsymbol{\theta} = \boldsymbol{\xi}_{wy} - \boldsymbol{\xi}_{\Delta w\Delta y}(\boldsymbol{\sigma}) \tag{13a}$$

where

$$\boldsymbol{R}_{\Delta w\Delta\varphi}(\boldsymbol{\sigma}) = \begin{bmatrix} \mathbf{0} & \mathbf{0} \\ \sigma_v \boldsymbol{I}_{n_a} & \mathbf{0} \\ \mathbf{0} & \sigma_i \boldsymbol{I}_{n_b} \\ \mathbf{0} & \mathbf{0} \end{bmatrix} \in \Re^{n_w \times n_\theta} \tag{13b}$$

$$\boldsymbol{\xi}_{\Delta w\Delta y}(\boldsymbol{\sigma}) = \begin{bmatrix} \sigma_v & \mathbf{0} & \mathbf{0} \end{bmatrix}^{\mathrm{T}} \in \Re^{n_w \times 1} \tag{13c}$$

The identification of overdetermined system (13a) boils down to a separable optimization problem:

$$\hat{\boldsymbol{\rho}} = \arg\min_{\boldsymbol{\rho}} \left\|\varepsilon(\boldsymbol{\rho})\right\|_2^2 \tag{14}$$

where $\boldsymbol{\rho}$ = [$\boldsymbol{\vartheta}^T$, $\boldsymbol{\sigma}^T$] with $\boldsymbol{\sigma}$ = [σ_v, σ_i]^T. The presented minimization problem can be solved by finding the global minimizer of the sum of squares of nonlinear residual ε. Referring to (13a) and assuming a known variance vector, the residual is easily written as:

$$\varepsilon(\boldsymbol{\theta}) = F(\boldsymbol{\sigma})\boldsymbol{\theta} - f(\boldsymbol{\sigma}) \tag{15a}$$

where

$$F(\boldsymbol{\sigma}) = \boldsymbol{R}_{w\varphi} - \boldsymbol{R}_{\Delta w\Delta\varphi} \tag{15b}$$

$$f(\boldsymbol{\sigma}) = \boldsymbol{\xi}_{wy} - \boldsymbol{\xi}_{\Delta w\Delta y} \tag{15c}$$

The presented minimization problem can be easily solved via the LS principle:

$$\hat{\boldsymbol{\theta}} = F^{+}(\hat{\boldsymbol{\sigma}})f(\hat{\boldsymbol{\sigma}}) \tag{16}$$

It is shown the noise variances are prerequisite for a unique solution of the model parameters. The variable projection algorithm (VPA) is applied here to extract the unknown variances. Substituting (16) into (15a) gives:

$$\begin{aligned} \hat{\boldsymbol{\sigma}} &= \arg\min_{\boldsymbol{\sigma}} \left\|\varepsilon(\boldsymbol{\sigma})\right\|_2^2 \\ &= \arg\min_{\boldsymbol{\sigma}} \left\|f(\boldsymbol{\sigma}) - F(\boldsymbol{\sigma})\boldsymbol{\theta}(\boldsymbol{\sigma})\right\|_2^2 \\ &= \arg\min_{\boldsymbol{\sigma}} \left\|[\boldsymbol{I} - F(\boldsymbol{\sigma})F^{+}(\boldsymbol{\sigma})]f(\boldsymbol{\sigma})\right\|_2^2 \end{aligned} \tag{17}$$

where $F(\sigma)F^{+}(\sigma)$ is the orthogonal projector on the range of $F(\sigma)$. The minimization problem can be solved by any optimization method in an offline manner.

Remark 1: The global minima of $\varepsilon(\boldsymbol{\vartheta}, \boldsymbol{\sigma})$ is the same with $\varepsilon(\boldsymbol{\sigma})$, i.e. $\left\|\varepsilon(\hat{\boldsymbol{\theta}}, \hat{\boldsymbol{\sigma}})\right\|_2^2 = \left\|\varepsilon(\hat{\boldsymbol{\sigma}})\right\|_2^2$. The dimension of the resulting minimization problem is hence reduced by applying VPA. This also lowers down the risk of being trapped in a local minimum.

Remark 2: Compared to minimizing Eq. (14), the VGA generally converges in less iterations.

Obviously the co-estimation problem can be solved via a two-step algorithm which solves Eq. (17) and then Eq. (16). Since the two equations are formulated with LS principle and VPA, the proposed method is shortened as LSVGA.

3.3 Online Version of LSVGA

The model parameters are expected to be online adapted due to their time-variant feature, so that an online version of the proposed LSVGA is favorable.

The minimization problem in Eq. (17) is solved iteratively via the Gauss-Newton (GN) method which facilitates online calculation. The GN-based LSVGA can be summarized into three steps as shown in Table 1.

Table 1 Procedures of the GN-based LSVGA

Define $\hat{\boldsymbol{\rho}}_k = \begin{bmatrix} \hat{\boldsymbol{\theta}}_k^T & \hat{\boldsymbol{\sigma}}_k^T \end{bmatrix}^T$ as the current solution.

Step 1: Solve the linear sub-problem:

$$\hat{\boldsymbol{\theta}}_{t,k} = F^{+}(\hat{\boldsymbol{\sigma}}_k)f(\hat{\boldsymbol{\sigma}}_k) \tag{18}$$

and set $\hat{\boldsymbol{\rho}}_{t,k} = \begin{bmatrix} \hat{\boldsymbol{\theta}}_{t,k}^T & \hat{\boldsymbol{\sigma}}_k^T \end{bmatrix}^T$.

Step 2: Compute the Gauss-Newton update direction $\boldsymbol{\mu}_k$ at $\hat{\boldsymbol{\rho}}_{t,k}$ by solving:

$$\hat{\boldsymbol{\mu}}_k = \arg\min_{\mu_k} \left\|J(\hat{\boldsymbol{\rho}}_{t,k})\boldsymbol{\mu}_k + \varepsilon(\hat{\boldsymbol{\rho}}_{t,k})\right\|_2^2 \tag{19}$$

where $J(\hat{\boldsymbol{\rho}}_{t,k})$ is the Jacobian matrix given by:

$$J(\hat{\boldsymbol{\rho}}_{t,k}) = \frac{\partial\varepsilon(\hat{\boldsymbol{\rho}}_{t,k})}{\partial\hat{\boldsymbol{\rho}}_{t,k}} = \begin{bmatrix} \dfrac{\partial\varepsilon(\hat{\boldsymbol{\rho}}_{t,k})}{\partial\hat{\boldsymbol{\theta}}_{t,k}} & \dfrac{\partial\varepsilon(\hat{\boldsymbol{\rho}}_{t,k})}{\partial\hat{\boldsymbol{\sigma}}_k} \end{bmatrix} \tag{20}$$

Step 3: Update the parameters and noise variances:

$$\hat{\boldsymbol{\rho}}_{k+1} = \hat{\boldsymbol{\rho}}_{t,k} - \hat{\boldsymbol{\mu}}_k\alpha_k \tag{21}$$

where α is the user-defined step size.

The entries of the $J(\hat{\boldsymbol{\rho}}_{t,k})$ are given by:

$$\frac{\partial\varepsilon(\hat{\boldsymbol{\rho}}_{t,k})}{\partial\hat{\boldsymbol{\theta}}_{t,k}} = F(\hat{\boldsymbol{\sigma}}_k) \tag{22a}$$

$$\frac{\partial \varepsilon(\hat{\boldsymbol{\rho}}_{t,k})}{\partial \hat{\boldsymbol{\sigma}}_k} = \frac{\partial F(\hat{\boldsymbol{\sigma}}_k)}{\partial \hat{\boldsymbol{\sigma}}_k}\hat{\boldsymbol{\theta}}_{t,k} - \frac{\partial f(\hat{\boldsymbol{\sigma}}_k)}{\partial \hat{\boldsymbol{\sigma}}_k} \tag{22b}$$

Note that the residual function is also linear in $\boldsymbol{\sigma}$, i.e.

$$\varepsilon(\hat{\boldsymbol{\rho}}_{t,k}) = G(\hat{\boldsymbol{\theta}}_{t,k})\hat{\boldsymbol{\sigma}}_k - g(\hat{\boldsymbol{\theta}}_{t,k}) \tag{23a}$$

where

$$G(\hat{\boldsymbol{\theta}}_{t,k}) = \boldsymbol{\xi}_{\Delta w \Delta y}(\hat{\boldsymbol{\sigma}}_k) - \boldsymbol{R}_{\Delta w \Delta \varphi}(\hat{\boldsymbol{\sigma}}_k)\hat{\boldsymbol{\theta}}_{t,k} = \begin{bmatrix} 1 & -\boldsymbol{a}_{t,k}^{\boldsymbol{T}} & \boldsymbol{0} & \boldsymbol{0} \\ 0 & \boldsymbol{0} & -\boldsymbol{b}_{t,k}^{\boldsymbol{T}} & \boldsymbol{0} \end{bmatrix}^{\mathrm{T}} \in \Re^{n_w \times 2} \tag{23b}$$

$$g(\hat{\boldsymbol{\theta}}_{t,k}) = \boldsymbol{\xi}_{wy} - \boldsymbol{R}_{w\varphi}\hat{\boldsymbol{\theta}}_{t,k} \tag{23c}$$

Equation (22b) hence simplifies to:

$$\frac{\partial \varepsilon(\hat{\boldsymbol{\rho}}_{t,k})}{\partial \hat{\boldsymbol{\sigma}}_k} = G\left(\hat{\boldsymbol{\theta}}_{t,k}\right) \tag{24}$$

Substituting Eq. (22a) and (24) into (20), then the optimization problem in Eq. (19) can be solved by:

$$\hat{\boldsymbol{\mu}}_k = J^{+}(\hat{\boldsymbol{\rho}}_{t,k})\varepsilon(\hat{\boldsymbol{\rho}}_{t,k}) \tag{25}$$

which completes the derivation of the GN-based LSVPA.

4. RESULTS AND DISCUSSION

4.1 Offline Identification

Periodical offline identification based on batch data is promising for model adaptation considering the potential use of cloud-based BMS. However, raw data collect from vehicle environment are featured with large disturbances. Hence, simulations are performed in this section to validate the proposed method for batch calculation. The first-order RC model in use is built in Matlab/Simulink, where model parameters are pre-defined to provide reference for the identified results. A hybrid pulse current is inputted to the model and the resulting voltages are sampled for offline model parameter extraction. With user-defined initial SOC, the reference of SOC and OCV can be known for validation. Random noises with different standard deviations (SDs) are added to the simulated signals.

The offline identification results by using commonly used LS and the proposed LSVPA are shown in Fig. 2. It is observed that LS gives obvious biased identification for all the parameters. The biases increase monotonously as the noise intensities enlarge. This is because the noise corruption on both system input and output violates the underlying assumption of LS. Moreover, the polarization impedances (R_p and C_p) are much more vulnerable to the disturbances than the ohmic resistance. Under a noise SD of 10 mV/mA, the biases of R_p and C_p reach up to 44.6% and 86.7%, respectively. By comparison, the proposed LSVPA can well compensate for the noise effect and identify the unknowns with much less biases. The ohmic resistance is identified quite accurately within the considered conditions, while the biases of R_p and C_p can be confined to 11.1% and 8.3% respectively.

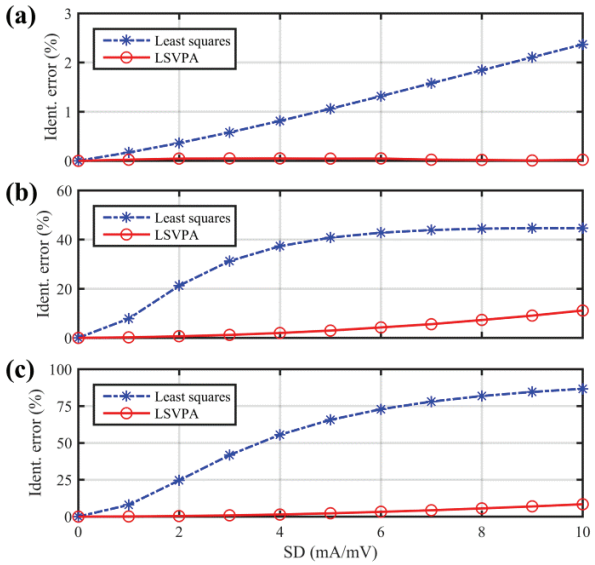

Fig. 2 Identification error of model parameters under different noise SDs: (a) R_s, (b) R_p, (c) C_p

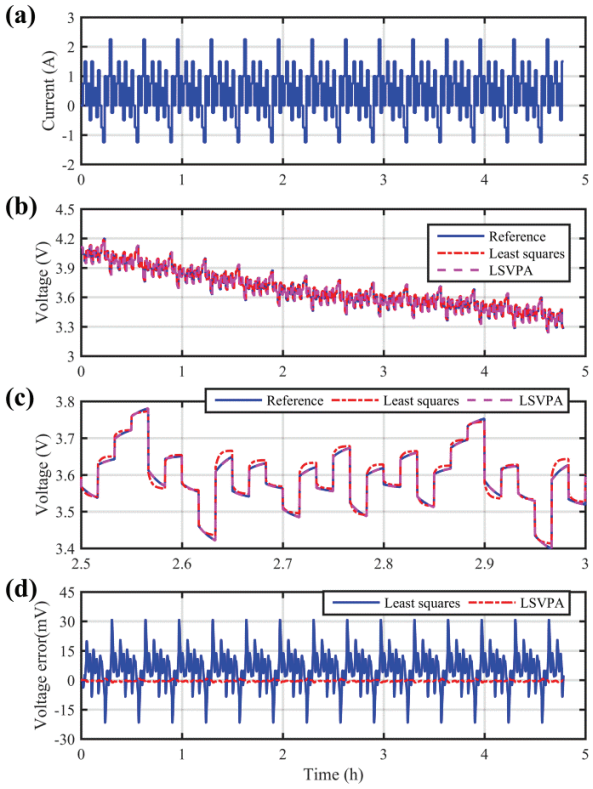

Fig. 3 Modeling results with LS and LSVPA used for parameterization: (a) load current, (b) predicted voltage, (c) zoom-in figure of (b), and (d) voltage prediction error

To give a more explicit description, the modeling results with LS and LSVPA used for parameterization under the noise SD of 10 mV/mA are plotted in Fig. 3. It is shown the model parameterized via LSVPA predicts the terminal voltage much more accurately than the LS-based model. This is within expectation as the model parameters which underlie the prediction accuracy have been identified with improved accuracy via the LSVPA.

4.2 Online Identification

An online recursive version of the LSVPA has been exploited via the Gauss-Newton method. In this section, experiments are performed on an 18650 NMC cell with nominal capacity of 2200 mAh to further validate the GN-based LSVPA. The hybrid pulse condition the same as in Fig. 3 (a) is imposed on the cell leveraging a battery cycler, inside which the ranges of sensors are 10 A and 5 V, while the error limits are both within 0.05%. As signals are sampled with accurate sensors under a well-protected lab environment, random noises with SDs of 10 mA and 2 mV are imposed on the measurements to simulate an environment with noise contamination.

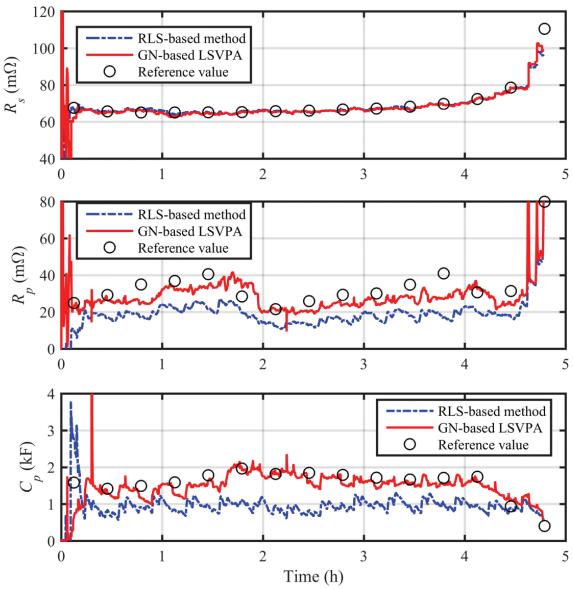

Fig. 4 Experimental results of online model identification

Note that the GN-based LSVPA needs the OCV to establish the regression model. Hence, an SOC observer is designed via pole placement and the estimated SOC is used to infer the OCV. The observer is integrated with the GN-based LSVPA in an interconnected framework to allow online model identification. The online identified model parameters along with their reference values are shown in Fig. 4. The reference model parameters explicitly show a time-variant and SOC-dependent feature, which validates the need of online parameter identification. The RLS-based method converges easily from the erroneous initialization, but substantial steady-state biases can be observed, especially for R_p and C_p. By comparison, the GN-based LSVPA keeps tracking the reference values with reduced biases, due to the merit of noise statistics estimate and noise effect compensation.

5. CONCLUSION

This paper aims for the noise-immune model identification for LIB. A novel LSVPA method is proposed to co-estimate the noise variances and unbiased model parameters. The GN-based LSVPA as a recursive version has also been put forward for real-time utilization. The proposed methods have been validated by both simulations and experiments. Results show that the proposed method well compensates for the noise effect and attenuates the identification biases caused by noise corruption. Comparison with the LS-based method further suggests the superiority of the proposed method in noise immunity and identification accuracy.

ACKNOWLEDGEMENT

This work is supported by the National Key R&D Program of China (No. 2018YFB0105900).

REFERENCE

[1] Wei Z, Zhao J, Ji D, Tseng KJ. A multi-timescale estimator for battery state of charge and capacity dual estimation based on an online identified model. Applied energy. 2017;204:1264-74.

[2] Kim T, Adhikaree A, Pandey R, Kang D, Kim M, Oh C-Y, et al. Outlier mining-based fault diagnosis for multiceli lithium-ion batteries using a low-priced microcontroller. 2018 IEEE Applied Power Electronics Conference and Exposition (APEC): IEEE; 2018. p. 3365-9.

[3] Zou C, Hu X, Wei Z, Wik T, Egardt B. Electrochemical estimation and control for lithium-ion battery health-aware fast charging. IEEE Transactions on Industrial Electronics. 2017;65:6635-45.

[4] Li Y, Vilathgamuwa M, Choi SS, Farrell TW, Tran NT, Teague J. Development of a degradation-conscious physics-based lithium-ion battery model for use in power system planning studies. Applied Energy. 2019;248:512-25.

[5] Chemali E, Kollmeyer PJ, Preindl M, Ahmed R, Emadi A. Long Short-Term Memory Networks for Accurate State-of-Charge Estimation of Li-ion Batteries. IEEE Transactions on Industrial Electronics. 2018;65:6730-9.
[6] Yu Z, Xiao L, Li H, Zhu X, Huai R. Model parameter identification for lithium batteries using the coevolutionary particle swarm optimization method. IEEE Trans Ind Electron. 2017;64:5690-700.
[7] Wang Y, Pan R, Liu C, Chen Z, Ling Q. Power capability evaluation for lithium iron phosphate batteries based on multi-parameter constraints estimation. Journal of Power Sources. 2018;374:12-23.
[8] Plett GL. Extended Kalman filtering for battery management systems of LiPB-based HEV battery packs: Part 2. Modeling and identification. Journal of power sources. 2004;134:262-76.
[9] Sitterly M, Wang L, Yin GG, Wang C. Enhanced Identification of Battery Models for Real-Time Battery Management. IEEE Transactions on Sustainable Energy. 2011;2:300-8.
[10] Wei Z, Zou C, Leng F, Soong BH, Tseng K-J. Online model identification and state-of-charge estimate for lithium-ion battery with a recursive total least squares-based observer. IEEE Transactions on Industrial Electronics. 2018;65:1336-46.
[11] Wei Z, Zhao J, Xiong R, Dong G, Pou J, Tseng KJ. Online Estimation of Power Capacity with Noise Effect Attenuation for Lithium-Ion Battery. IEEE Transactions on Industrial Electronics. 2018.
[12] Arablouei R, Doğançay K, Adalı T. Unbiased recursive least-squares estimation utilizing dichotomous coordinate-descent iterations. IEEE transactions on signal processing. 2014;62:2973-83.